Id: 6775
Au: Saper, R.; Xu, G.; Kux, Hermann J.H.
Ti: SAR range resolution and the detection of forest clearings.
Anais. 1993. p.393-398 p. 6

Co: Apresentado em: Canadian Symposium on Remote Sensing, 16; Quebec, 07-10 jun. 1993.
Pr: DSM.
Lo: INPE-9092-PRE/1092.

16^e Symposium canadien sur la télédétection
16th Canadian Symposium on Remote Sensing
8^e Congrès de L'Association québécoise de télédétection

SAR RANGE RESOLUTION AND THE DETECTION OF FOREST CLEARINGS

Ron Saper, Vantage Point International, 1324 Cedarcroft Cres., Gloucester, Ontario, CANADA, K1B 5C8, Tel. (613) 747-0118, Fax (613) 747-0940

George Xu, Canada Centre for Remote Sensing, 588 Booth Street, Ottawa, Ontario, CANADA, K1A 0Y7, Tel. (613) 947-1305, Fax (613) 947-1385

Hermann Kux, INPE, C.P. 515, 12201 S. José Dos Campos - S.P., BRAZIL, Tel. 55-123-418977, Fax 55-123-218743

ABSTRACT

It is demonstrated that the detection of forest clearings can be enhanced by improved range resolution. Modest improvements in range resolution make spaceborne synthetic aperture radar systems much more useful for detection and mapping of forest clear-cut boundaries.

RÉSUMÉ

Il est démontré que la détection des zones d'éclaircies en forêt peut être améliorée par l'amélioration de la résolution en portée latérale. Des améliorations modestes dans la résolution en portée latérale rendent beaucoup plus utiles les systèmes satellitaires radar à antenne synthétique pour la détection et la cartographie des limites de coupes en forêt.

INTRODUCTION

The thesis of this paper is that range resolution is a critical parameter affecting the detectibility of both the dark near-edge and bright far-edge of forest clear-cuts in synthetic aperture radar (SAR) images. Renewed consideration should be given to range resolution performance when selecting a platform for the clear-cut boundary mapping application or when specifying future systems for this application.

Mapping of forest clear-cuts with satellite imagery is an important application of remote sensing to forestry because of the potential for efficient clear-cut inventory under all weather conditions. Many technical challenges remain for SAR clear-cut mapping. Recent ERS-1 SAR imagery of the forest area near Whitecourt, Alberta, shows no evidence of existing clear-cuts. Although the steep incidence angle of ERS-1 has previously been blamed for the absence of clear-cut features, we will show that range resolution also plays a vital role.

In general, radar shadow and bright returns are present at the near and far edges respectively of a clear-cut when illuminated by a SAR. The shadow at the near edge results from an absence of scattering at the ranges represented, while the bright return at the far edge is caused mainly by strong corner reflection of microwaves from the ground and tree trunks. The presence of radar shadow and bright return in a forest clear-cut scene helps to delineate clear-cut boundaries. Any enhancement of these phenomena will hence improve mapping accuracy and reliability.

If a radar shadow is present, it must be at least as large as the height of the object which is casting the shadow. Thus, *sufficiently fine range resolution will detect any shadow regardless of the incidence angle.*

Discrete scatterers such as trunk-ground corner reflectors occupy a small physical area assumed to fall within a single resolution cell. Improvements in range resolution reduce the dimensions of each resolution cell and thus reduce the power in surrounding cells relative to the cell containing the discrete scatterer.

RADAR RANGE RESOLUTION

Range resolution is defined as the minimum separation of two point objects in range where they may just barely be recognized as distinct. The radar range resolution ρ_r is often defined by

$$\rho_r = \frac{c\tau_{eff}}{2} \tag{1}$$

where $c = 3 \times 10^8$ m/s is the speed of light, and τ_{eff} is the effective pulse width.[1] Equation 1 reflects the simple idea that the radar returns from two point objects will be distinct if they do not overlap in time.

Often range resolution is specified as the projection of the true range resolution onto a flat or spheroidal surface. This is called the *ground range resolution*, ρ_{gr}, defined as

$$\rho_{gr} = \frac{\rho_r}{\sin\theta} \tag{2}$$

Note that ρ_{gr} varies with incidence angle. Using equation 2 one can readily derive the more fundamental *slant range resolution* ρ_r from ρ_{gr} and a nominal incidence angle θ.

RADAR SHADOW AT THE NEAR EDGE

Figure 1 shows a schematic profile of the near edge of an idealized forest clear-cut. The edge is modelled as a vertical step in a microwave-opaque surface. The range length of the shadow L is dependent upon the height of the trees h and the incidence angle θ as follows:

$$L = \frac{h}{\cos\theta} \tag{3}$$

As θ approaches 90°, the shadow becomes longer. For θ near zero, the shadow length L approaches h. It is therefore apparent that a (slant) range resolution of less than the height of the trees can ensure that the radar shadow will be resolved by the SAR.

Surprisingly, the slant range resolutions for spaceborne SARs are usually much better than the commonly quoted ground range resolutions. We shall see that RADARSAT should be capable of discerning many near edge boundaries and that, for sufficiently tall trees such as those found in Amazonia, the range resolution of ERS-1 is adequate to detect radar shadow at some near-edge boundaries.

BRIGHT RETURNS AT THE FAR EDGE

The bright return from a discrete scatterer will be visible if the backscattered power it contributes can compete with the power from distributed scatterers within the resolution cell. If so, the "target" will stand out from the "clutter" in surrounding cells. We arbitrarily define a ratio of the power from the discrete "target" to the power from the "clutter" in the resolution cell:

$$\Omega = \frac{S_{discrete}}{S_{clutter}} \tag{4}$$

Using any of several forms of the well-known radar equation (Skolnik, 1980), we can show that Ω may be expressed as:

$$\Omega = \frac{\sigma_{discrete}}{A_{cell}\sigma_0} \tag{5}$$

---

[1] In most modern SARs the effective pulse width is much shorter than the physical pulse width due to the use of *pulse compression* techniques.

where $\sigma_{discrete}$ is the radar cross section of the discrete scatterer, σ_0 is the radar cross section per unit area for the surrounding clutter, and A_{cell} is the ground area of the resolution cell which is defined as

$$A_{cell} = \frac{\rho_r \rho_{az}}{\sin\theta} \tag{6}$$

where ρ_{az} is the SAR resolution in the azimuth direction. Thus an improvement in range resolution produces a proportional reduction in resolution cell size and an improvement in Ω.

IMPLICATIONS FOR SOME SAR SENSORS

Salient parameters for several modes of the Canada Centre for Remote Sensing's C/X SAR, for ERS-1 and for three sub-modes of RADARSAT are summarized in Table 1. (CCRS,1988; Attema:1991; CSA:1992). In RADARSAT's standard mode, beams 1 and 2 have a different ρ_r from beams 3-5, an expedient to ensure roughly square resolution cells.

Using equation 3 we can predict the height at which the length of the radar shadow equals the resolution limit for each of the SAR platforms in the table. These minimum ideal-edge tree height thresholds for discernable shadow are tabulated in Table 2. It is advisable to add a 50-100% margin to arrive at detectable heights since the resolution definition is defined for barely distinguishable separations, and since the edge of a clear-cut may be far from ideal.

SAREX DATA FROM AMAZONIA

The data shown here was collected as part of the Tropical Forestry Initiative (TFI), a joint project between the Canada Centre for Remote Sensing (CCRS) and INPE, the Brazilian Institute for Space Research. The Canadian International Development Agency provided financial support for the TFI.

The study site is Lowland Tropical Rainforest with bamboo frequently dominating, and is located in the Acre State, Western Amazonia, Brazil. The crown of some species, such as the well-known "Castanheira" (Brazil-nut), can exceed a height of 50 m above the soil. A more detailed description of the area under study is the subject of another paper (Kux et al. 1993).

Figure 2 is a portion of a C-VV image from the CCRS C/X airborne SAR in its wide swath mode. The SAR illuminates from the right, θ = 77° at the cut, and the maximum length of the shadow in slant range was estimated at between 150 and 190 m. The slant range resolution of the C/X SAR in wide mode is 20 m, therefore the shadow is visible. Using equation 3, we estimate a tree height of between 33 and 43 m, which is reasonable for the area in question though ground data is not yet available. Bright returns from trunk-ground structures are evident in this image, so presumably Ω is significantly greater than one.

Figure 3 shows the same clear-cut imaged by ERS-1. The look direction is from the right, illuminating the cut area from a similar but not identical angle. At the cut θ=24° and the maximum slant-range length of the shadow was estimated at between 20 and 36 m. The slant-range resolution of ERS-1 is 9.6 m, therefore the shadow is visible, although at low contrast.

Using equation 3, we estimate a tree height of between 18 and 33 m, somewhat less than the estimate obtained using Figure 2. Bright returns at the far edge are absent, presumably due to the larger resolution cell area noted in Table 1, an absence of strong discrete scatterers at ERS-1 incidence angles, or both.

CONCLUSIONS

The analysis presented here illuminates mechanisms for cut boundary detection and gives a basis for understanding when and why these mechanisms become significant. The discrepancy in tree height estimate results for ERS-1 and the C/X SAR is likely due to a non-ideal cut boundary. Rounding of the crown top and regrowth at the base of the cut would cause a shorter effective tree height at small incidence angles.

The implications are encouraging for the clear-cut mapping application. RADARSAT's fine mode will probably detect near-edge boundaries for trees on the order of 10 m in height. Its small resolution cell area should also improve detectibility of the far edge. One obvious caveat is that RADARSAT's fine mode is a single look mode, and as such will have elevated speckle. Table 2 shows that RADARSAT's standard modes, unfortunately, are unlikely to be any better than ERS-1 for clear-cut boundary mapping using edge features.

Experiments are needed to validate the feasibility of mapping clear-cuts using edge features. Tree height and cut edge profile data must be collected for a given study site and, where multiple SARs are used, the look directions should be the same. A range of incidence angles and resolution modes could be used. The potential of RADARSAT's fine mode for clear-cut boundary mapping should be verified early in the lifetime of that satellite so that operational potential can be evaluated.

ACKNOWLEDGEMENT

The authors gratefully acknowledge the assistance of Dr Frank Ahern of CCRS and Ron Pietsch of Dendron Resource Surveys in reviewing this paper and preparing the figures respectively.

REFERENCES

Attema, E.P.W 1991. The Active Microwave Instrument On-Board the ERS-1 Satellite. *Proc. of the IEEE*, vol. 79, no. 6, pp 791-799.

Canada Centre for Remote Sensing 1988. The Airborne C/X SAR. *Technical Brochure.*

Canadian Space Agency, 1992. CDPF Presentation to CCRS RDDP Participants, *Copies of Presentation Overheads.*

Kux, H.J.H., F.J. Ahern, R.K. Raney, R.W. Pietsch & B. Tittley, 1993. The Contribution of SAREX'92 (South American Radar Experiment) Campaign to the Evaluation of Natural Resources in Tropical Rainforests: First Results from Test Site Acre, SW Amazonia, Brazil. *16th Canadian Symposium on Remote Sensing,* Sherbrooke, Québec.

Skolnik, M.I. 1980. Introduction to Radar Systems. *McGraw-Hill Inc,* New York, pp 15-65.

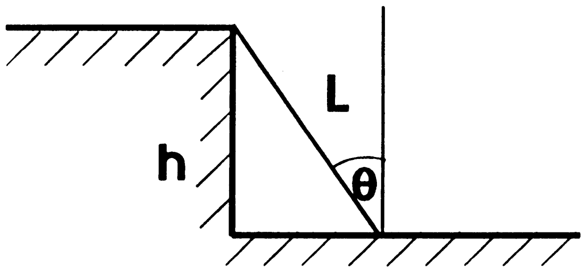

Figure 1 Model of the near edge of the clear-cut.

Figure 2. Airborne SAR image of clear-cut.

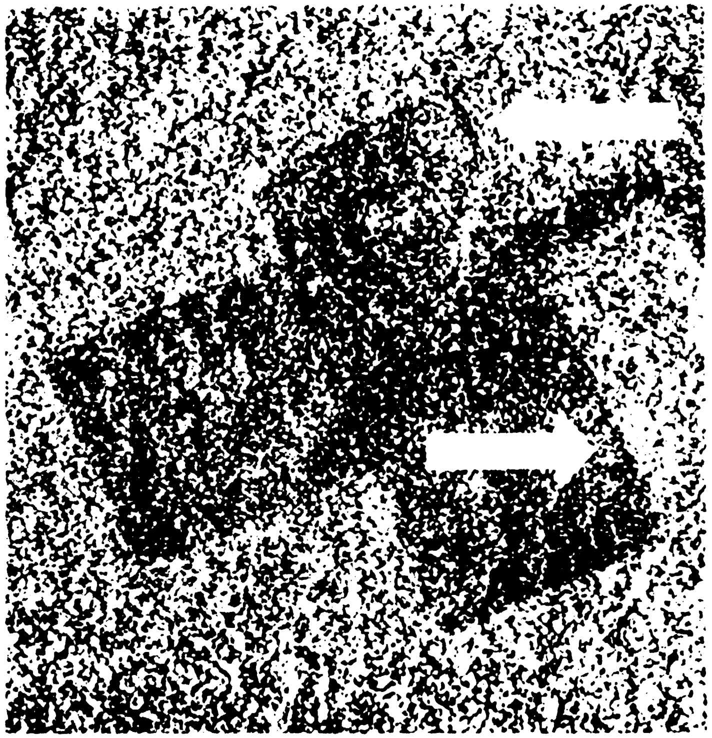

Figure 3. ERS-1 SAR image of clear-cut.

TABLE 1. SAR Parameters.

SAR Platform and Mode	ρ_r	A_{cell}	θ
C/X SAR, Narrow Mode	6 m	51 m² - 37 m²	45° - 76°
C/X SAR, Nadir Mode	6 m	1400 m² - 37 m²	0° - 74°
C/X SAR, Wide Mode	20 m	280 m² - 200 m²	45° - 85°
ERS-1 SGF Product	9.6 m	730 m² (Nominal)	23° (Nominal)
RADARSAT Fine Beams SGF Product	5.7 m	80 m² - 64 m²	37° - 48°
RADARSAT Standard Beam 1 SGF Product	10.3 m	710 m² (Nominal)	23° (Nominal)
RADARSAT Standard Beam 5 SGF Product	15.3 m	570 m² (Nominal)	47° (Nominal)

TABLE 2. Minimum Ideal Edge Tree Height Threshold

SAR Platform and Mode	Min. Tree Height
C/X SAR, Narrow Mode	4.2 m
C/X SAR, Nadir Mode	6.0 m
C/X SAR, Wide Mode	14 m
ERS-1 SGF Product	8.8 m
RADARSAT Fine Mode	4.6 m
RADARSAT Standard Beam 1 SGF Product	9.5 m
RADARSAT Standard Beam 5 SGF Product	10 m